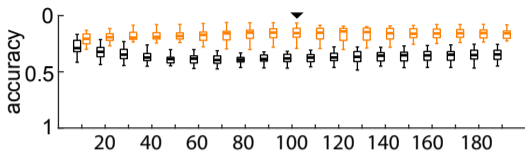
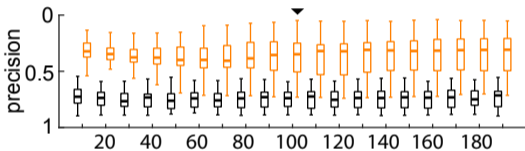
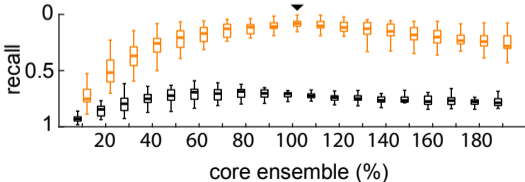
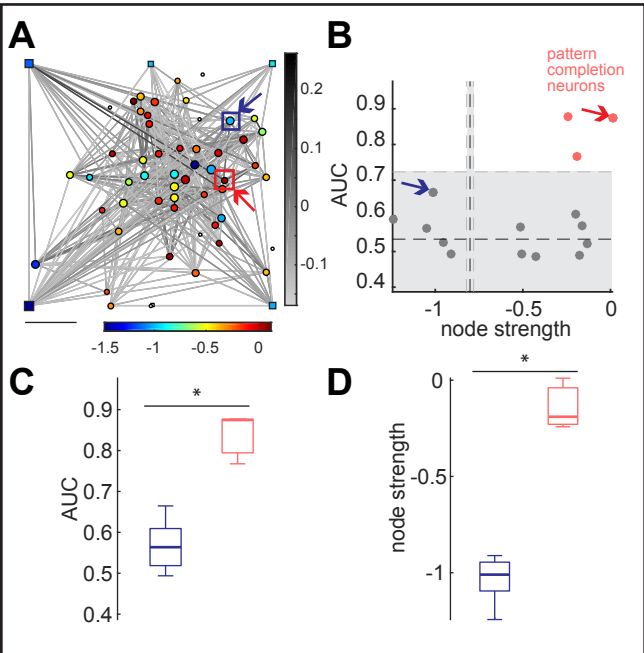
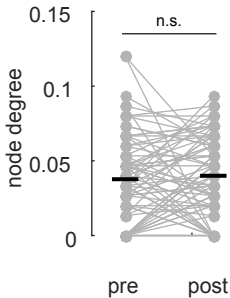
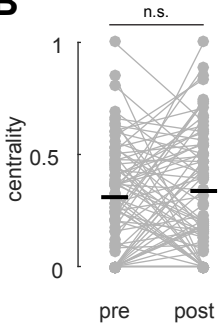
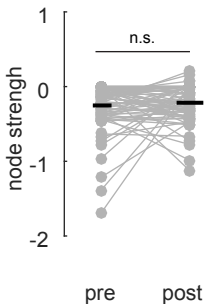
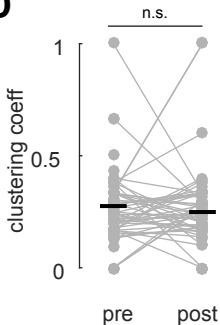


**A****B****C**



**A****B****C****D**

## Supplementary Information

### Figure S1. CRF models with added nodes recapitulate the same properties of baseline CRF models

**A.** CRF graphs of baseline model (no added nodes) and the added node model, trained with the same experimental data. Edge color represents strength of node potentials ( $\phi_{11}$ ); node color represents node strength. Node size represents node degree. Scale bar: 50 $\mu$ m. **B.** Graph density (P=0.4375 n.s), **C.** node strength (P=0.8438 n.s), **D.** node degree (P=0.1563 n.s), **E.** clustering coefficient (P=0.1563 n.s) and **G.** centrality (P=0.5625 n.s) values between baseline and added node models (n = 6 mice; Wilcoxon signed rank test). Each dot in the data plots represents the mean value for a different mouse. Related to Figure 2.

### Figure S2. Core ensembles from CRF have the highest classification performance for visual stimuli

**A.** Accuracy, **B.** precision and **C.** recall for classification performance from randomly down-sampled or up-sampled CRF core ensembles (orange). Randomly chosen ensembles are represented in black. Data presented as box and whisker plots displaying median and interquartile ranges (n = 6 mice; Wilcoxon rank sum test). Related to Figure 4.

### Figure S3. Identification of neurons from CRF models with pattern completion capability

**A.** CRF graphical model from simultaneous two-photon imaging and two-photon optogenetic single cell stimulation after imprinting protocol. Squares depict added nodes representing stimulation trials from 6 different neurons. Edge color tone represents edge potential strength ( $\phi_{11}$ ); node color represents node strength. Scale bar: 50 $\mu$ m. **B.** Neurons with pattern completion capability defined by AUC values and node strength are depicted in red. AUC values were calculated by predicting the photostimulation time of targeted neurons with single cell resolution using the cosine similarity function of core ensemble population vectors from the imprinted ensemble. Optogenetically targeted neurons are highlighted by arrows (Red: neuron with pattern completion capability; blue: neuron without pattern completion capability). Dashed line and grey region represent confidence interval calculated from random groups of neurons. **C.** AUC values (P=0.0357\*) and **D.** node strength (P=0.0357\*) of neurons with (red) and without (blue) pattern completion capability inferred with CRF graphical models. Note that two-photon optogenetic

photostimulation of neurons with pattern completion capability (red) was able to recall imprinted ensembles whereas single cell stimulation of other neurons (blue) was not able to induce pattern completion of imprinted ensembles. Data presented as box and whisker plots displaying median and interquartile ranges (Wilcoxon rank sum test). Related to Figure 5.

**Figure S4. Global network properties of cortical microcircuits remain stable after two-photon optogenetic stimulation**

**A.** Node strength ( $P=0.9733$  n.s), **B.** node degree ( $P=0.2921$  n.s), **C.** clustering coefficients ( $P=0.7022$  n.s) and **D.** centrality ( $P=0.4225$  n.s) values of non-stimulated neurons. Note that the whole network remains stable after ensemble imprinting. Data plots represent photostimulated neurons activated by imprinting protocol. ( $n=74$  neurons; Wilcoxon signed rank test). Related to Figure 5.